Bivalent, Trivalent, and Tetravalent Nickel Complexes with a Common Tridentate Deprotonated Pyridine Bis-Amide Ligand. Molecular Structures of Nickel(II) and Nickel(IV) and Redox Activity

Apurba Kumar Patra and Rabindranath Mukherjee*

Department of Chemistry, Indian Institute of Technology, Kanpur 208 016, India

Received June 16, 1998

Using a tridentate bis-amide ligand 2,6-bis[*N*-(phenyl)carbamoyl]pyridine (H_2L), in its deprotonated form, nickel complexes in three consecutive oxidation states $[Et_4N]_2[Ni^{II}L_2]\cdot H_2O$ (**1**), $[Et_4N][Ni^{III}L_2]\cdot H_2O$ (**2**), and $[Ni^{IV}L_2]\cdot 0.75H_2O$ (**3**) have been prepared, and **1** and **3** structurally characterized. These X-ray structures represent first crystallographically characterized NiN_6 coordination sphere, with a common pyridine bis-amide ligand. Complex **1** crystallizes in the orthorhombic space group *Pccn*, $a = 10.175(2)$ Å, $b = 20.834(3)$ Å, $c = 23.765(4)$ Å, $Z = 4$, and **3** crystallizes in the monoclinic space group $P2_1/a$, $a = 14.874(7)$ Å, $b = 13.300(4)$ Å, $c = 16.604(5)$ Å, $\beta = 99.678(3)°$, $Z = 4$. Considerable distortion is observed with the average distances being $Ni-N_{amide}$ 2.131(8) Å and $Ni-N_{py}$ 1.994(7) Å for **1** and $Ni-N_{amide}$ 1.946(8) Å and $Ni-N_{py}$ 1.846(8) Å for **3**. The observation of short axial $M-N_{py}$ and long equatorial $M-N_{amide}$ bonds (tetragonally compressed octahedral geometry) is caused by the steric requirement of the ligand. Magnetic susceptibility measurements (63−300 K) reveal that the spin states of nickel centers in **1** and **2** are $S = 1$ and $S = {}^1/_2$, respectively. Complex **3** is diamagnetic. In their absorption spectra (MeCN), **1** exhibits a d−d transition at 854 nm; **2** and **3** display LMCT transitions at 449 nm with a shoulder at 636 nm and at 480 nm with a shoulder at 730 nm, respectively. The nickel(III) complex **2** exhibits a rhombic EPR signal (*g* values: 2.149, 2.115, and 2.034), showing that the metal center is the primary residence site of the unpaired electron. Cyclic voltammetric measurements of **1** in MeCN solution at a glassy carbon electrode exhibit two chemically reversible ($i_{p,a}/i_{p,c} \approx 1$) and electrochemically quasireversible ($\Delta E_p = 100$ mV) oxidative responses: a $Ni^{III}-Ni^{II}$ couple ($E_{1/2} = 0.05$ V vs SCE) and a $Ni^{IV}-Ni^{III}$ couple ($E_{1/2} = 0.51$ V vs SCE). A one-electron chemical oxidation of yellowish brown **1** was achieved in a two-phase solvent mixture $H_2O-CH_2Cl_2$ with $[Fe(\eta^5\text{-}C_5H_5)_2][PF_6]$, which led to the isolation of reddish brown **2**. A two-electron chemical oxidation of **1** was readily achieved in MeCN with ceric ammonium nitrate to afford dark violet crystals of **3**. For **1** a linear correlation between the $Ni^{III}-Ni^{II}$ reduction potentials and the reciprocal of solvent dielectric constants is obtained.

Introduction

Stabilization of nickel in its higher (>2) oxidation state[1−3] was a challenge to inorganic chemists during seventies and eighties. The ligands used to fulfill the electronic requirements of Ni(III) or Ni(IV) states were primarily oximes[1−6] or deprotonated amides.[7−9] In recent years, synthesis of trivalent nickel complexes[10−12] has attracted attention to bioinorganic chemists to provide models,[11,12] for the Ni sites in [NiFe]-hydrogenases.[13]

It has been well-documented that amidato-*N* ligands[7,14,15] have the ability to stabilize high formal oxidation states of metal ions, due to their good σ-donor properties of the deprotonated nitrogen. Since strong donor ligands reduce the oxidizing properties of high-valent complexes,[15] salicylamide[15,16] and pyridine amide[17−22] ligands which resist oxidative degradation, afford very stable (characterized by X-ray crystallography) complexes with a wide range of metal ions. Very recently, we found[23] that simple, easily synthesizable, tridentate dianionic bis-amide ligand L(2−) [H_2L = 2,6-bis(*N*-phenylcarbamoyl)-

(1) (a) Nag, K.; Chakravorty, A. *Coord. Chem. Rev.* **1980**, *33*, 87. (b) Chakravorty, A. *Isr. J. Chem.* **1985**, *25*, 99.
(2) Haines, R. I.; McAuley, A. *Coord. Chem. Rev.* **1981**, *39*, 77.
(3) Lappin, A. G.; McAuley, A. *Adv. Inorg. Chem.* **1988**, *32*, 241.
(4) (a) Baucom, E. I.; Drago, R. S. *J. Am. Chem. Soc.* **1971**, *93*, 6469. (b) Sproul, G.; Stucky, G. D. *Inorg. Chem.* **1973**, *12*, 2898.
(5) Drago, R. S.; Baucom, E. I. *Inorg. Chem.* **1972**, *11*, 2064.
(6) (a) Panda, R. K.; Acharya, S.; Neogi, G.; Ramaswamy, D. *J. Chem. Soc., Dalton Trans.* **1983**, 1225. (b) Bemtgen, J.-M.; Gimpert, H.-R.; von Zelewsky, A. *Inorg. Chem.* **1983**, *22*, 3576.
(7) Margerum, D. W. *Pure Appl. Chem.* **1983**, *55*, 23.
(8) (a) Bossu, F. P.; Margerum, D. W. *J. Am. Chem. Soc.* **1976**, *98*, 4003. (b) Bossu, F. P.; Margerum, D. W. *Inorg. Chem.* **1977**, *16*, 1210. (c) Lappin, A. G.; Murray, C. K.; Margerum, D. W. *Inorg. Chem.* **1978**, *17*, 1630. (d) Jacobs, S. A.; Margerum, D. W. *Inorg. Chem.* **1984**, *23*, 1195.
(9) (a) Sugiura, Y.; Mino, Y. *Inorg. Chem.* **1979**, *18*, 1336. (b) Sakurai, T.; Hongo, J.-I.; Nakahara, A.; Nakao, Y. *Inorg. Chim. Acta* **1980**, *46*, 205.
(10) Collins, T. J.; Nichols, T. N.; Uffelman, E. S. *J. Am. Chem. Soc.* **1991**, *113*, 4708.
(11) (a) Krüger, H.-J.; Holm, R. H. *Inorg. Chem.* **1987**, *26*, 3645. (b) Krüger, H.-J.; Holm, R. H. *J. Am. Chem. Soc.* **1990**, *112*, 2955. (c) Krüger, H.-J.; Peng, G.; Holm, R. H. *Inorg. Chem.* **1991**, *30*, 734.
(12) (a) Baidya, N.; Olmstead, M. M.; Mascharak, P. K. *J. Am. Chem. Soc.* **1992**, *114*, 9666. (b) Marganian, C. A.; Vazir, H.; Baidya, N.; Olmstead, M. M.; Mascharak, P. K. *J. Am. Chem. Soc.* **1995**, *117*, 1584 and references therein.
(13) (a) Cammack, R. *Adv. Inorg. Chem.* **1988**, *32*, 297. (b) Moura, J. J. G.; Moura, I.; Teixeira, M.; Xavier, A. V.; Fauque, G. D.; Legall, J. *Met. Ions Biol. Syst.* **1988**, *23*, 285.
(14) Sigel, H.; Martin, R. B. *Chem. Rev.* **1982**, *82*, 385.
(15) Collins, T. J. *Acc. Chem. Res.* **1994**, *27*, 279 and references therein.
(16) (a) Koikawa, M.; Gotoh, M.; Ōkawa, H.; Kida, S.; Kohzuma, T. *J. Chem. Soc., Dalton Trans.* **1989**, 1613. (b) Koikawa, M.; Ōkawa, H.; Maeda, Y.; Kida, S. *Inorg. Chim. Acta* **1992**, *194*, 75.
(17) (a) Mulqi, M.; Stephens, F. S.; Vagg, R. S. *Inorg. Chim. Acta* **1981**, *52*, 73. (b) Stephens, F. S.; Vagg, R. S. *Inorg. Chim. Acta* **1982**, *57*, 9. (c) Stephens, F. S.; Vagg, R. S. *Inorg. Chim. Acta* **1986**, *120*, 165. (d) Kawamoto, T.; Hammes, B. S.; Ostrander, R.; Rheingold, A. L.; Borovik, A. S. *Inorg. Chem.* **1998**, *37*, 3424.

10.1021/ic980672e CCC: $18.00
Published on Web 03/13/1999

pyridine] is capable of stabilizing trivalent state of iron and

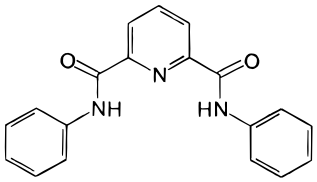

H_2L

cobalt to a considerable extent, in their bis-chelate complexes. Most interestingly, these low-spin complexes exhibit tetragonal distortion with two unusually short axial bonds. The present work stems from our search for preparing nickel analogues using L(2−) in unusual stereochemistry and high oxidation state.

Here we report the synthesis and characterization of highly stable nickel complexes in all the three oxidation states, $[Et_4N]_2[Ni^{II}L_2]\cdot H_2O$ (**1**), $[Et_4N][Ni^{III}L_2]\cdot H_2O$ (**2**), and $[Ni^{IV}L_2]\cdot 0.75H_2O$ (**3**). This work presents, to the best of our knowledge, the first structural study on tetragonally compressed nickel(II) complex **1** as well as nickel(IV) complex **3**, with a common deprotonated amide ligand L(2−), providing NiN_6 coordination sphere. The present comparative studies offer the first direct evidence for the influence of coordination geometry on the electrochemical behavior of Ni(II), Ni(III), and Ni(IV), with a given bis-amide ligand.

Experimental Section

Materials and Reagents. All chemicals were obtained from commercial sources and used as received. Solvents were dried/purified as reported previously.[23] The ligand 2,6-bis(*N*-phenylcarbamoyl)pyridine and tetra-*n*-butylammonium perchlorate (TBAP) were prepared as before.[23] $[Fe(\eta^5\text{-}C_5H_5)_2][PF_6]$ was prepared following a reported procedure.[24]

Synthesis of Metal Complexes. (a) $[Et_4N]_2[NiL_2]\cdot H_2O$ (1). The ligand H_2L (100 mg, 0.315 mmol) was dissolved in dinitrogen flushed *N*,*N*′-dimethylformamide (DMF) (5 mL) and to it was added solid NaH (35 mg, 1.46 mmol), resulting in a light yellow solution. $NiCl_2\cdot 6H_2O$ (40 mg, 0.168 mmol) was dissolved in DMF (5 mL) separately. The latter solution was then added to the ligand solution using a cannula under a dinitrogen atmosphere. The resulting brownish yellow solution was magnetically stirred for 2 h at 298 K in the air. To this was added solid $[Et_4N]Cl\cdot xH_2O$ (111 mg, 0.67 mmol), and stirring was continued for 12 h. Removal of the solvent was followed by addition of MeCN (10 mL) and filtration. Reducing the volume of the solution down to ∼3 mL and addition of diethyl ether (∼8 mL) to it resulted in the crystallization of a dark brownish yellow compound (90 mg; ∼56%). Recrystallization from MeCN−EtOAc (vapor diffusion) afforded crystalline solid suitable for structural studies.

Characterization. Anal. Calcd for $C_{54}H_{68}N_8O_5Ni$: C, 67.03; H, 7.03; N, 11.59. Found: C, 66.98; H, 6.99; N, 11.56. Conductivity (MeCN; 10^{-3} M solution at 298 K): $\Lambda_M = 222$; (in DMF) 121; (in DMSO) 65; (in H_2O) 272 Ω^{-1} cm^2 mol^{-1}. Absorption spectrum [λ_{max}, nm (ϵ, M^{-1} cm^{-1}): (in MeCN) 225 sh (52 640), 249 (38 000), 286 sh (30 100), 352 sh (8070), 854 (87); (in DMF) 375 sh (8170), 480 (790), 863 (85); (in DMSO) 857 (93); (in H_2O) 815 (145)].

(b) $[Et_4N][NiL_2]\cdot H_2O$ (2). To a magnetically stirred solution of $[Et_4N]_2[NiL_2]\cdot H_2O$ (50 mg, 0.052 mmol) in distilled water (1 mL) was added solid $[Fe(\eta^5\text{-}C_5H_5)_2][PF_6]$ (20.5 mg, 0.062 mmol) followed by immediate addition of CH_2Cl_2 (25 mL). The reddish-brown reaction mixture thus formed was stirred for 30 min. The CH_2Cl_2 layer was then separated. The water layer was washed with CH_2Cl_2 (2 × 5 mL) and all of the CH_2Cl_2 extracts were then collected. After addition of anhydrous Na_2SO_4 it was left for 3 h. After removal of inorganic solid the filtrate was concentrated to ∼1−2 mL. Addition of EtOAc (∼3 mL) precipitated a brown microcrystalline compound. The solid was collected by filtration, washed with EtOAc, and finally with diethyl ether. This crude product was contaminated with $[Et_4N][PF_6]$. Recrystallization was achieved by vapor diffusion of diethyl ether into an MeCN solution to afford highly crystalline brown compound (yield: 16 mg, ∼38%).

Characterization. Anal. Calcd for $C_{46}H_{48}N_7O_5Ni$: C, 65.97; H, 5.74; N, 11.71. Found: C, 65.87; H, 5.80; N, 11.68. Conductivity (MeCN, 10^{-3} M solution at 298 K): $\Lambda_M = 165$ Ω^{-1} cm^2 mol^{-1}. Absorption spectrum [λ_{max}, nm (ϵ, M^{-1} cm^{-1}): (in MeCN) 275 sh (20 320), 304 (17 000), 449 (7140), 636 sh (1960)].

(c) $[NiL_2]\cdot 0.75\ H_2O$ (3). A solution of $[Et_4N]_2[NiL_2]\cdot H_2O$ (45 mg, 0.047 mmol) in MeCN (1 mL) was added dropwise to a stirred solution of $[NH_4]_2[Ce(NO_3)_6]$ (75 mg, 0.137 mmol) within a time span of 15 min. The violet colored microcrystalline compound started precipitating out. The mixture was stirred for a further 45 min and then filtered. The collected solid was washed with cold MeCN (1 mL). Recrystallization was achieved by diethyl ether diffusion into a $CHCl_3$ solution of the complex. Block-like single crystals were formed which were filtered and vacuum-dried (yield: 22 mg, ∼61%).

Characterization. Anal. Calcd for $C_{38}H_{27.5}N_6O_{4.75}Ni$: C, 64.94; H, 3.92; N, 11.96. Found: C, 64.91; H, 3.93; N, 12.00. Conductivity (MeCN, 10^{-3} M solution at 298 K): $\Lambda_M = 15$ Ω^{-1} cm^2 mol^{-1}. Absorption spectrum [λ_{max}, nm (ϵ, M^{-1} cm^{-1}): (in MeCN) 299 sh (11 770), 480 (13 700), 730 sh (4820)].

Physical Measurements. Solution electrical conductivity measurements were carried out with an Elico (Hyderabad, India) Type CM-82 T conductivity bridge. Spectroscopic data were obtained by using the following instruments: infrared spectra, Perkin-Elmer M-1320; electronic spectra, Perkin-Elmer Lambda 2; X-band EPR spectra, Varian E−109 C; ^{1}H NMR spectra, Brüker WP-80 (80 MHz) NMR spectrometer.

Variable-temperature (63−300 K) solid-state magnetic susceptibility measurements were done by the Faraday technique using a locally built magnetometer.[23] The set up consists of an electromagnet with constant gradient pole caps (Polytronic Corporation, Mumbai, India), Sartorius M25-D/S balance (Germany), a closed cycle refrigerator, and a Lake Shore temperature controller (Cryo Industries, USA). All measurements were made at a fixed main field strength of ∼10 kG. Solution-state magnetic susceptibility was obtained by the NMR technique of Evans[25] in MeCN with a PMX- 60 JEOL (60 MHz) NMR spectrometer. Susceptibilities were corrected for diamagnetic contribution which was calculated to be -388×10^{-6} cm^3 mol^{-1} for **1** and -276×10^{-6} cm^3 mol^{-1} for **2** by using literature values.[26]

(18) (a) Che, C.-M.; Ma, Ji-X.; Wong, W.-T.; Lai, T.-F.; Poon, C.-K. *Inorg. Chem.* **1988**, *27*, 2547. (b) Mak, S.-T.; Yam, V. W.-W.; Che, C.-M. *J. Chem. Soc., Dalton Trans.* **1990**, 2555. (c) Mak, S.-T.; Wong, W.-T.; Yam, V. W.-W.; Lai, T.-F.; Che, C.-M. *J. Chem. Soc., Dalton Trans.* **1991**, 1915. (d) Che, C.-M.; Leung, W.-H.; Li, C.-K.; Cheng, H.-Y.; Peng, S.-M. *Inorg. Chim. Acta* **1992**, *196*, 43. (e) Ko, P.-H.; Chen, T.-Y.; Zhu, J.; Cheng, K.-F.; Peng, S.-M.; Che, C.-M. *J. Chem. Soc., Dalton Trans.* **1995**, 2215 and references therein.

(19) (a) Yang, Y.; Diederich, F.; Valentine, J. S. *J. Am. Chem. Soc.* **1991**, *113*, 7195. (b) Wocadlo, S.; Massa, W.; Folgado, J.-V. *Inorg. Chim. Acta* **1993**, *207*, 199 and references therein.

(20) (a) Ray, M.; Mukherjee, R.; Richardson, J. F.; Buchanan, R. M. *J. Chem. Soc., Dalton Trans.* **1993**, 2451. (b) Ray, M.; Mukherjee, R.; Richardson, J. F.; Mashuta, M. S.; Buchanan, R. M. *J. Chem. Soc., Dalton Trans.* **1994**, 965 and references therein.

(21) (a) Brown, S. J.; Tao, X.; Stephan, D. W.; Mascharak, P. K. *Inorg. Chem.* **1986**, *25*, 3377. (b) Tao, X.; Stephan, D. W.; Mascharak, P. K. *Inorg. Chem.* **1987**, *26*, 754. (c) Delany, K.; Arora, S. K.; Mascharak, P. K. *Inorg. Chem.* **1988**, *27*, 705. (d) Chavez, F. A.; Olmstead, M. M.; Mascharak, P. K. *Inorg. Chem.* **1996**, *35*, 1410. (e) Chavez, F. A.; Nguyen, C. V.; Olmstead, M. M.; Mascharak, P. K. *Inorg. Chem.* **1996**, *35*, 6282.

(22) Redmore, S. M.; Rickard, C. E. F.; Webb, S. J.; Wright, L. J. *Inorg. Chem.* **1997**, *36*, 4743.

(23) Ray, M.; Ghosh, D.; Shirin, Z.; Mukherjee, R. *Inorg. Chem.* **1997**, *36*, 3568 and references therein.

(24) Ercolani, C.; Gardini, M.; Pennesi, G.; Rossi, G.; Russo, U. *Inorg. Chem.* **1988**, *27*, 422.

(25) Evans, D. F. *J. Chem. Soc.* **1959**, 2003.

(26) O'Connor, C. J. *Prog. Inorg. Chem.* **1982**, *29*, 203.

Table 1. Crystal Data for $[Et_4N]_2[NiL_2]\cdot H_2O$ (**1**) and $[NiL_2]\cdot 0.75H_2O$ (**3**)

	1	**3**
empirical formula	$C_{54}H_{68}N_8O_5Ni$	$C_{38}H_{27.5}N_6O_{4.75}Ni$
fw	966.69	702.19
temp. (°C)	20	20
radiation (λ, Å)	Mo Kα (0.710 73)	Mo Kα (0.710 73)
space group	*Pccn* (No. 56)	$P2_1/a$ (No. 14)
a, Å	10.175(2)	14.874(7)
b, Å	20.834(3)	13.300(4)
c, Å	23.765(4)	16.604(5)
β, deg		99.678(3)
V, Å^3	5037.85(1)	3237.93(2)
Z	4	4
ρ (calcd), g cm^{-3}	1.276	1.443
μ (Mo Kα), mm^{-1}	0.44	0.65
$R(F_o)^a$	0.069	0.061
$R_w(F_o)^b$	0.044	0.064

^{a} $R = \sum(F_o - F_c)/\sum F_o$. ^{b} $R_w = [\sum w(F_o - F_c)^2/\sum wF_o^2]^{1/2}$, $w = 1/\sigma(F)$.

Cyclic voltammetric measurements were performed by using a PAR model 370 electrochemistry system, consisting of a model 174A polarographic analyzer with a model 175 universal programmer. A PAR model G0021 glassy carbon electrode was used as the working electrode. All potentials were measured referenced to the saturated calomel electrode (SCE) at 298 K; no corrections were made for junction potentials.

Crystal Structure Determinations. A yellow block-shaped crystal of $[Et_4N]_2[NiL_2]\cdot H_2O$ **1** (dimensions: 0.3 × 0.2 × 0.1 mm) and blue well-formed crystal of $[NiL_2]\cdot 0.75H_2O$ **3** (dimensions: 0.2 × 0.2 × 0.1 mm) were used for data collection. Diffracted intensities were collected on an Enraf Nonius CAD4-Mach diffractometer using graphite-monochromated Mo Kα radiation (λ = 0.710 73 Å). Lattice parameters for the complex was obtained from least-squares analyses of 25 machine-centered reflections. Three standard reflections were measured at every hour to monitor instrument and crystal stability. Intensity data were corrected for Lorentz and polarization effects; analytical absorption corrections were applied. The XTAL3.2 program package[27] was used in absorption and all subsequent calculations. The linear absorption coefficients, neutral atom scattering factors for the atoms, and anomalous dispersion corrections for non-hydrogen atoms were taken from ref 28. The structures were solved by the direct method and successive difference Fourier syntheses. The function minimized during full-matrix least-squares refinement was $\sum w(F_o - F_c)^2$ where $w = 1/\sigma(F)$. The hydrogen atoms of the water molecules were located by a Fourier difference map. The positions of the hydrogen atoms were calculated assuming ideal geometries of the atom concerned and their positions and thermal parameters were not refined. All other atoms were refined with anisotropic thermal parameters. Crystal data and a summary of experimental results are presented in Table 1. Selected bond distances and angles are listed in Table 2. The rest of the crystallographic data have been submitted as Supporting Information.

Results and Discussion

Synthesis. The synthesis of the nickel(II) compound $[Et_4N]_2[NiL_2]\cdot H_2O$ **1** involved initial anaerobic reaction of Na_2L with $NiCl_2\cdot 6H_2O$ in DMF at 298 K to form a brownish yellow complex. Addition of $[Et_4N]Cl\cdot xH_2O$ and usual workup afforded yellow air-stable crystals. Clean one-electron chemical oxidation of **1** in 1:25 $H_2O-CH_2Cl_2$ solvent mixture (v/v) by 1.2 equiv of $[Fe(\eta^5\text{-}C_5H_5)_2][PF_6]$ generated a reddish brown solution, which on usual workup led to the isolation of the nickel(III) complex, $[Et_4N][NiL_2]\cdot H_2O$ (**2**). When the chemical oxidation of **1** was performed in MeCN using 3.0 equiv of ceric ammonium nitrate a net two-electron oxidation occurred, resulting in the generation of a violet solution. Usual workup of this solution produced dark violet microcrystals of the nickel(IV) complex $[NiL_2]\cdot 0.75\ H_2O$ **3**. The absence of ν(N−H) in the IR spectra of **1**−**3** confirmed that the ligand is coordinated in the deprotonated form. For all the three complexes ν(OH) absorption of water of crystallization was observed in the region 3400−3500 cm^{-1}. Elemental analyses, IR, and solution electrical conductivity data (**1**, 1:2 electrolyte; **2**, 1:1 electrolyte; **3**, nonelectrolyte in MeCN)[29] are in agreement with the above formulations.

Table 2. Selected Bond Lengths (Å) and Angles (deg) of $[Et_4N]_2[NiL_2]\cdot H_2O$ (**1**) and $[NiL_2]\cdot 0.75H_2O$ (**3**)

1		**3**	
Ni−N(1)	2.127(8)	Ni−N(1)	1.940(7)
Ni−N(2)	1.994(7)	Ni−N(2)	1.852(8)
Ni−N(3)	2.135(8)	Ni−N(3)	1.953(7)
		Ni−N(4)	1.949(8)
		Ni−N(5)	1.840(8)
		Ni−N(6)	1.942(8)
N(1)−Ni−N(2)	76.0(3)	N(1)−Ni−N(2)	81.9(3)
N(1)−Ni−N(2′)	100.8(3)	N(1)−Ni−N(3)	164.3(3)
N(1)−Ni−N(3)	153.5(3)	N(1)−Ni−N(4)	90.4(3)
N(1)−Ni−N(3′)	97.2(3)	N(1)−Ni−N(5)	98.2(3)
N(2)−Ni−N(3)	77.6(3)	N(1)−Ni−N(6)	91.7(3)
N(2)−Ni−N(3′)	105.7(3)	N(2)−Ni−N(3)	82.4(3)
N(1)−Ni−N(1′)	89.2(3)	N(2)−Ni−N(4)	97.2(3)
N(2)−Ni−N(2′)	175.6(4)	N(2)−Ni−N(5)	179.8(4)
N(3)−Ni−N(3′)	88.4(3)	N(2)−Ni−N(6)	97.5(3)
		N(3)−Ni−N(4)	90.6(3)
		N(3)−Ni−N(5)	97.4(3)
		N(3)−Ni−N(6)	91.2(3)
		N(4)−Ni−N(5)	82.7(3)
		N(4)−Ni−N(6)	165.3(3)
		N(5)−Ni−N(6)	82.6(3)

Among polarizable anionic ligands known to stabilize high oxidation states of nickel, deprotonated oximes deserve special mention. Chakravorty and co-workers prepared Ni(II), Ni(III), and Ni(IV) complexes with NiN_6 coordination sphere using tridentate and hexadentate amino-imino-oxime ligands.[1−3] From the standpoint of present investigation, the complexes with pyridine-2,6-bis(acetyloxime) (H_2dapo) reported by Drago et al. are worth mentioning.[4] This ligand forms six-coordinate Ni(II) and Ni(IV) complexes, which are isolated in the solid state. The structure of the Ni(IV) complex $[Ni(dapo)_2]$ has been demonstrated crystallographically. Holm et al.[11b] demonstrated the existence of the intermediate Ni(III) species, $[Ni(dapo)_2]^-$ from coulometric generation and subsequent characterization by EPR spectroscopy.

Description of the Structures. (a) $[Et_4N]_2[NiL_2]\cdot H_2O$ (1). A view of the anion is presented in Figure 1. The nickel center is coordinated to two L(2−) ligands. The Ni atom sits on an imposed C_2 axis and is coordinated by four deprotonated amide nitrogens in the equatorial plane [N(1) and N(3) and their symmetry related] and two pyridyl nitrogens [N(2) and its symmetry related] in the axial positions. The Ni atom is constrained by symmetry to lie on the equatorial plane. The arrangement of the ligands in **1** is meridional, as that observed with its Fe(III) and cobalt(III) analogues, $[Et_4N][FeL_2]\cdot 1.5H_2O$ and $[Et_4N][CoL_2]\cdot 2H_2O$.[23]

The geometry of the $Ni^{II}N_6$ coordination polyhedron is appreciably compressed octahedral (Table 2). Significant deviation from 90° of the bond angles involving the chelation is

(27) Hall, S. R.; Flack, H. D.; Stewart, J. M. (Eds.) *The XTAL 3.2 Reference Manual*; Universities of Western Australia, Geneva, and Maryland: 1992.

(28) *International Tables for X-ray Crystallography*; Kynoch Press: Birmingham, England, 1974; Vol. IV.

(29) Geary, W. J. *Coord. Chem. Rev.* **1971**, *7*, 81.

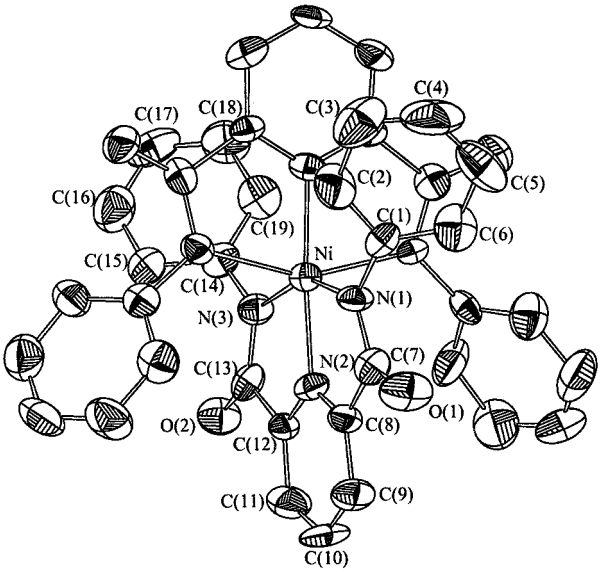

Figure 1. View of the molecular structure of the anion of $[Et_4N]_2[NiL_2]\cdot H_2O$ (**1**), showing atom-labeling scheme and 50% probability ellipsoids. Hydrogen atoms are omitted for clarity. Unlabeled atoms are related to labeled atoms by the crystallographic 2-fold axis.

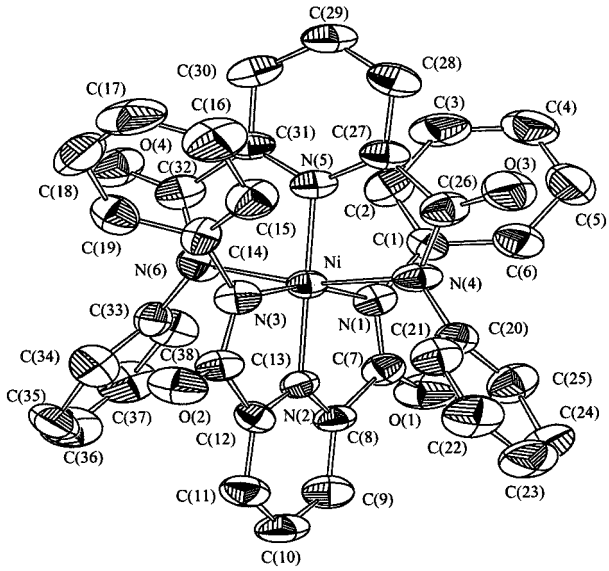

Figure 2. View of the metal coordination environment in the crystal of $[NiL_2]\cdot 0.75H_2O$ (**3**), showing atom-labeling scheme and 50% probability ellipsoids. Hydrogen atoms are omitted for clarity.

observed (Table 2) presumably due to formation of five-membered chelate rings with extended conjugation, as observed for the bis-chelates of iron(III) and cobalt(III).[23] Further evidence of strain in the chelate rings arises from the following observation. Though in each ligand the two *N*-phenyl rings and the pyridine ring are planar, the two phenyl rings, however, make an angle of ∼56° to each other and angles of ∼122° and ∼129° with the central pyridine ring.

The average $Ni^{II}-N_{amide}$ distance in **1** (2.131 Å) is appreciably longer, compared to those in square-planar Ni(II) complexes with pyridine amide ligands (1.839−1.918 Å).[17] A very interesting feature of this structure is the Ni^{II}-N_{py} bond length (1.994 Å), which is appreciably shorter (∼0.05 Å) than that observed for $[Et_4N]_2[Ni^{II}(pdtc)_2]$ (pdtc = pyridine-2,6-(monothiocarboxylate)(2−)), with NiN_4S_2 coordination sphere.[11b] It is worth noting here that the $Ni^{II}-N_{py}$ bond lengths for the square planar $Ni^{II}N_4$ complexes with pyridine amide ligands span in the range 1.944−1.960 Å.[17a−c] Due to the strong donor capacity of deprotonated amide N donors providing four negative charges on the equatorial plane, it is expected to have shorter $Ni-N_{amide}$ bond lengths. The opposite effect observed here is the result of steric predominance over electronic effect, as observed for Fe(III) and Co(III) complexes of L(2−).[23] A similar situation with exceptionally short $Ni^{II}-N_{py}$ bond distance of 1.805 Å has recently been reported for a square planar pyridyl diamide complex with $Ni^{II}N_3O$ coordination sphere.[17d]

(b) $[NiL_2]\cdot 0.75H_2O$ (3). A view of the metal environment in **3** is shown in Figure 2. To the best of our knowledge, it is the first crystallographically characterized neutral six-coordinate nickel(IV) complex with a deprotonated amide ligand. Comparing the molecular structures of **1** and **3** it is revealed that the coordination environment around nickel centers is closely similar. The average $Ni-N_{py}$ distances 1.994 Å for **1** and 1.846 Å for **3** and $Ni-N_{amide}$ distances 2.131 Å for **1** and 1.946 Å for **3** are clearly distinguishable. The $Ni-N_{py}$ bond length of **3** can be compared with $Ni(dapo)_2$ having $Ni^{IV}N_6$ coordination sphere. The bond length for the present complex is shorter by ∼0.13 Å.[4b] This significant difference in bonding parameters adds credence to our +4 oxidation state assignment of nickel in **3**. As that in **1**, though in each ligand the two *N*-phenyl rings and the pyridine ring are planar, the two phenyl rings, however, make an angle of ∼66° to each other and angles of ∼104° and ∼97° with the central pyridine ring for one ligand; for the other ligand the two phenyl rings make an angle of ∼109° to each other and angles of ∼104° and ∼85° with the central pyridine ring.

Interestingly, in **3** all the C−O bond lengths are not similar. For one ligand the average distance is 1.22 Å, but for the other the distances are dissimilar. In fact, one distance is 1.21 Å and the other is slightly longer 1.23 Å, implying a partial single bond character (the normal range of bond lengths are C═O (≈1.20 Å) and C−O (≈1.43 Å)).[30] For an N-coordinated and therefore deprotonated amide group it is expected that the negative charge would be delocalized along the amide C−N and C−O bonds, leading to two resonance forms which have

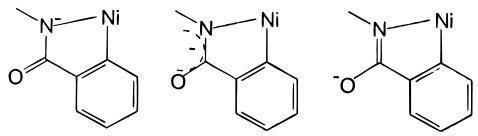

different C−N and C−O bond lengths. In resonance form I, C−N has single-bond character, C−O has double-bond character, and the $Ni-N_{amide}$ bond is expected to be relatively short. Conversely, in resonance form II, C−N has double bond character, C−O single bond character and the $Ni-N_{amide}$ bond is expected to be longer. These bonds can also be intermediate between double and single bonds. Out of four $Ni-N_{amide}$ bonds, one ligand gives distances of 1.942 and 1.949 Å and the other ligand gives distances of 1.940 and 1.953 Å. The evidence for the presence of a partial negative charge on the amide oxygen O(3) (the one which gives rise to $Ni-N_{amide}$ bond length of 1.953 Å) **3** comes from the presence of a hydrogen-bonded water molecule, in close proximity. The O(1w)···O(3) distance of 2.96 (2) Å is typical of systems with strong hydrogen-bonding, O−H···O.[30b]

(30) (a) Machida, R.; Kimura, E.; Kushi, Y. *Inorg. Chem.* **1986**, *25*, 3461. (b) McLachlan, G. A.; Brudenell, S. J.; Fallon, G. D.; Martin, R. L.; Spiccia, L.; Tiekink, E. R. T. *J. Chem. Soc., Dalton Trans.* **1995**, 439.

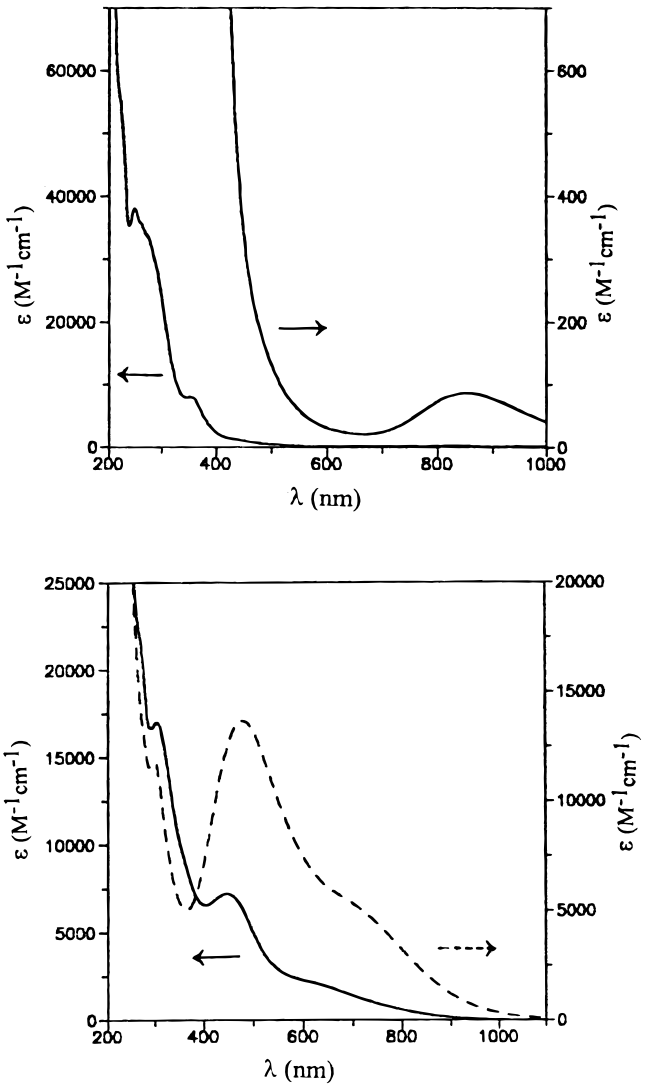

Figure 3. Electronic absorption spectra of $[Et_4N]_2[NiL_2]\cdot H_2O$ (**1**) (top) and $[Et_4N][NiL_2]\cdot H_2O$ (**2**) (solid line) and $[NiL_2]\cdot 0.75H_2O$ (**3**) (dashed line) in MeCN solutions.

Absorption Spectra. The absorption spectra of **1**−**3** in MeCN are displayed in Figure 3. It is the easiest means of their characterization. The yellowish orange solution of the Ni(II) complex **1** exhibits a crystal field transition at 854 nm, which could be assigned as ν_1 band ($^3A_{2g} \rightarrow {}^3T_{2g}$ in octahedral parentage). This feature remains invariant to change in solvents such as DMF, DMSO, and water. The reddish brown Ni(III) complex **2** is characterized by its LMCT transition at 449 nm with a shoulder at 636 nm. The spectrum of **3** is dominated by the intense LMCT band at 480 nm with a shoulder at 730 nm, which accounts for the violet color of the complex.

Ground States of $[NiL_2]^z$. (a) $[NiL_2]^{-2}$. The effective magnetic moment of **1** in MeCN solution is 3.09 μ_B (300 K), corresponding to an $S = 1$ state, with an appreciable orbital contribution.[31] The magnetism of its polycrystalline Et_4N^+ salt was investigated over the temperature range 63−300 K to define the spin-state and allow structural inferences. The compound follows the Curie−Weiss law. The magnetic moment value of 3.12 μ_B at 300 K of polycrystalline **1** is in conformity with the solution-state data.

(b) $[NiL_2]^-$. Because we were unable to grow single crystals for this compound, structural information is lacking. Hence we have investigated its temperature-dependent magnetic susceptibility behavior. The effective magnetic moment of **2** in the solid-state at 300 K was 2.14 μ_B, attesting the presence of only one unpaired electron with appreciable orbital contribution.[31] The result followed the Curie−Weiss law. In MeCN solution (300 K), $\mu_{eff} = 2.16\ \mu_B$.

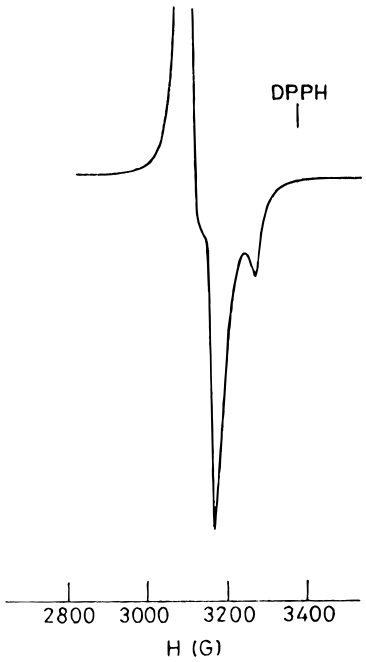

Figure 4. EPR spectrum of a polycrystalline sample of **2** at 77 K.

To clarify the ambiguous situation between nickel(II)-stabilized ligand radicals and authentic nickel(III) complexes, EPR spectral behavior of **2** was investigated. Solid samples of **2** at 300 K exhibits predominantly an axial spectrum with $g_\perp = 2.129$ and $g_\parallel = 2.049$. However, at 77 K the spectrum is cleanly rhombic with three principal g values of 2.149, 2.115, and 2.034 (Figure 4). The average g value ($g_{av} = 2.100$) indicates that the unpaired electron is associated primarily with the nickel ion. If ligand oxidation had occurred, as is a possibility given the electrochemical behavior of $[M^{III}L_2]^-$ (M = Fe, Co),[23] the paramagnetic product would be a nitrogen- or carbon-centered radical complex of nickel(II). Such species would be expected to exhibit g values close to the spin-only value of 2.002. The large orbital contribution to paramagnetism actually observed suggests that the unpaired electron is located primarily on the metal ion consistent with the trivalent oxidation state. The nature of the observed nonaxial spectrum strongly suggests that the rhombic field splits the perpendicular absorption into overlapping g_{xx} and g_{yy} components, the corresponding parallel absorption being represented by g_{zz}. Hence we can write "$g_\parallel$" = 2.034 and "$g_\perp$" = $^1/_2(g_{xx} + g_{yy}) = 2.132$. The spectral characteristics is closely similar to that observed for $Ni(bpyO_2)_3^{3+}$ ($bpyO_2$ = 2,2′-bipyridine 1,1′-dioxide).[32] The present behavior with $g_\perp > g_\parallel$ is consistent with a d_{z^2} ground state in a tetragonally distorted octahedral geometry with elongation of the axial bonds.[1−3] This is in sharp contrast to what we have observed (tetragonal compression) in the X-ray structures of Ni(II) and Ni(IV) complexes (vide supra). Thus on removal of an electron from a Ni(II) complex **1** there is a structural change. In frozen MeCN solution the spectrum is isotropic ($g = 2.113$).

(c) $[NiL_2]$. In $CDCl_3$ solution complex **3** displays a clean ^1H NMR spectrum (Figure S1, Supporting Information) closely

(31) Drago, R. S. In *Physical Methods in Chemistry*; Saunders: Philadelphia, 1977; Chapter 11, pp 411−435.

(32) Bhattacharya, S.; Mukherjee, R.; Chakravorty, A. *Inorg. Chem.* **1986**, *25*, 3448.

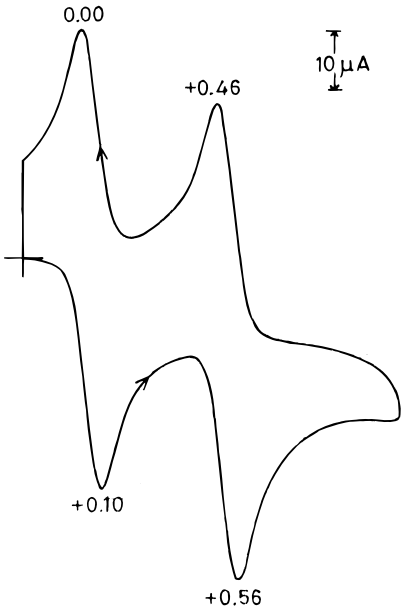

Figure 5. Cyclic voltammogram (50 mV/s) of a 1.03 mM solution of $[Et_4N]_2[NiL_2]\cdot H_2O$ (**1**) at a glassy carbon electrode in acetonitrile (0.15 M in TBAP).

similar to that observed for $[Co^{III}L_2]^-$,[23] attesting its diamagnetic ground state.

Redox Properties. (a) Electron-Transfer Reactions. To investigate the extent of stabilization of the nickel(II) state toward oxidation and whether a possibility corresponding to the accessibility of higher oxidation states could be achieved, cyclic voltammetric (CV) studies on **1** were performed.

CV scan of **1** in MeCN at a glassy carbon electrode shows two consecutive quasireversible couples at $E_{1/2} = 0.05$ and 0.51 V vs SCE, with ΔE_p values of 100 mV (Figure 5). The one-electron nature of each redox response has been confirmed by comparison of current height[23] with the redox response of a sample of $[Et_4N][FeL_2]\cdot 1.5H_2O$, under the same experimental conditions. The pertinent redox couples are represented in the following electron-transfer series (eq 1).

$$[Ni^{IV}L_2] \underset{-e^-}{\overset{+e^-}{\rightleftharpoons}} [Ni^{III}L_2]^- \underset{-e^-}{\overset{+e^-}{\rightleftharpoons}} [Ni^{II}L_2]^{2-} \qquad (1)$$

The observation of two clean well-separated oxidative redox responses was the key to our choice of chemical oxidizing agents in the successful isolation of nickel(III) as well as nickel(IV) complexes **2** and **3**.

CV studies on isolated nickel(III) and nickel(IV) complexes **2** and **3** exhibit identical behavior to that observed for complex **1**. This documents the purity and authenticity of the isolated nickel(III) and nickel(IV) complexes. The observed stabilizing potential of L(2−) toward Ni(III) and Ni(IV) states must be due to the presence of four deprotonated amide nitrogen coordination.

Within NiN_6 family of complexes with amide ligands, to the best of our knowledge, the present $Ni^{III}-Ni^{II}$ potential is the lowest.[1−3] It is worth mentioning here that the nickel(IV) complex of Chakravorty et al. undergoes two successive one-electron reductions in MeCN, with the $Ni^{III/II}$ potential at −0.20 V and Ni^{IV}/Ni^{III} potential at 0.30 V vs SCE.[1b]

(b) Solvent Dependency of the Redox Processes. Due to its ready solubility in many solvents we investigated the redox behavior of **1** as a function of solvent: MeCN, DMF, DMSO, and water. In going from DMF to water, an appreciable anodic shift (270 mV) in the $E_{1/2}$ value for the $Ni^{III}-Ni^{II}$ couple is observed.[33] It is worth noting here that, though a similar trend was observed, the $E_{1/2}$ value for the $Fe^{III}-Fe^{II}$ couple of $[FeL_2]^-$, however, shifts more anodically. This investigation reveals that the Ni(II) state of the complex $[NiL_2]^{2-}$ is systematically better stabilized due to enhanced solvation, as the dielectric constant of the medium is increased. Interestingly, the $Ni^{III}-Ni^{II}$ reduction potentials correlate linearly with inverse of the dielectric constant of the medium (Figure S2, Supporting Information), in line with the free energy of solvation as predicted by the Born equation.[34] A similar plot was obtained for $[Fe^{III}L_2]^-$.[23]

Summary

The following are the principal findings and conclusions of this investigation.

(1) To the best of our knowledge, this report documents the first examples of synthesis and characterization of nickel complexes in three oxidation states +2, +3, and +4 with a common deprotonated bis-amide ligand.

(2) The X-ray structures of nickel(II) and nickel(IV) complexes reveal that in both the cases the metal ion is coordinated in tetragonally compressed geometry with four comparatively longer $Ni-N_{amide}$ distances and two very short $Ni-N_{py}$ bonds. The two-electron oxidation of a Ni(II) complex **1** to a Ni(IV) complex **3** is accompanied by an expected decrease in the Ni−N bond lengths, as revealed by X-ray structural analysis.

(3) The Ni(II) complex **1** is paramagnetic with respect to two unpaired electrons ($S = 1$). The Ni(III) complex **2** has $S = {}^1/_2$ state, as determined by temperature-dependent magnetic susceptibility. EPR spectroscopy reveals that the unpaired electron is in a d_{z^2} orbital, suggesting tetragonally elongated geometry of the Ni(III) state. The Ni(IV) complex **3** is diamagnetic.

(4) Redox properties of these complexes unravel the attainment of a three-member electron-transfer series with oxidation states of nickel shuttling between +2, +3, and +4. This unique property of clean redox transformations has allowed us to synthesize genuine Ni(III) and Ni(IV) complexes. The $E_{1/2}$ values for the $Ni^{III}-Ni^{II}$ redox process (0.05 V vs SCE) as well as $Ni^{IV}-Ni^{III}$ process (0.51 V vs SCE) are apparently the lowest for a NiN_6 complex having deprotonated amide coordination.

(5) Due to their fascinating redox properties, easily synthesizable high-valent nickel complexes **2** and **3**, are ideally suited to be used as one-electon and two-electron potent outer-sphere oxidants, respectively.

Acknowledgment. This work is supported by grants from the Council of Scientific & Industrial Research (CSIR) and Department of Science and Technology (DST), Government of India, New Delhi. The financial assistance of the National X-ray diffractometer facility by DST at this Department is gratefully acknowledged.

Supporting Information Available: Experimental details and crystallographic structure determination information for **1** and **3**, in CIF format (Table S1−S16), magnetic data for **1** and **2** (Tables S17 and S18), ^1H NMR spectrum of **3** in $CDCl_3$ (Figure S1), and least-squares plot of $E_{1/2}$ ($Ni^{III}-Ni^{II}$) of **1** vs reciprocal of dielectric constant of the solvents (Figure S2). This material is available free of charge via the Internet at http://pubs.acs.org.

IC980672E

(33) The shift in the $Ni^{IV}-Ni^{III}$ couple does not follow any trend: 0.66 V (water), 0.58 V (DMSO), 0.51 V (MeCN), 0.58 V (DMF).

(34) Sawyer, D. T.; Roberts, J. L., Jr. *Experimental Electrochemistry for Chemists*; Wiley: New York, 1974; pp 186, 204−207.